J. Phys. Earth, **20**, 341-356, 1972

MODEL SEISMOLOGY ON A DIPPING LAYER

Tameshige TSUKUDA

Geophysical Institute, Faculty of Science, Universiiy of Tokyo, Tokyo

(Received December 28, 1972)

Recent developments in the study of crustal response to seismic waves it have necessitated research on the effect of an inclined or a concaved interface of discontinuity in the crust or upper mantle structure. In this paper, the effect of the inclination on the observed spectrum at the surface is examined by an experimental method (two-dimensional model seismology).

Ray-theoretical consideration is found to be valid even for dip angles as large as 30°. We can readily explain the main features of recorded waves and their spectra (or the transfer functions) in terms of the following properties: multiple reflections within a dipping layer; conversions between P and S phases at the free surface and at the bottom boundary of the layer; polarities of S waves.

It has been experimentally established that dip angles of the layer of less than about 5°-10°, the amplitude characteristics of the transfer functions show only slight changes in forms and in peak frequencies.

The key point of the experiment for studying the effects of a dipping layer on the transfer function is the generation of plane waves. For this purpose, many sources of cylindrical waves are used taking advantange of the superposition principle.

1. *Introduction*

The frequency response of the crustal layers to teleseismic waves has been an important subject in seismology. This response is often called the transfer function of the crust. A model of the crust, usually constructed with stratified layers, enables us to use the Thomson-Haskell matrix method in calculating theoretical transfer functions. This theory is applied to many problems that are related to crustal response.

The transfer function method is particularly helpful in revealing crustal structures. For instance, PHINNEY (1964) worked out a solution to the above problem, utilizing a spectral ratio of the vertical component to the horizontal motion observed at a free surface.

In geophysical researches the transfer function is sometimes employed to determine the crustal structure. Using the trial-and-error method, a comparison is made between the observational and theoretical characteristic curves. In this process the prominent peaks and troughs of the two amplitude characteristic curves should be fitted accurately because the spacing of some peaks and troughs reflect the depth of a certain interface of discontinuity. Furthermore, the difference between the peak and the trough amplitude is dependent on the sharpness of such a discontinuity.

The positions of the peaks in a frequency characteristic curve may also be affected

by an inclination of the interface because of variations in the arrival times of multiply reflected pulses. The effect of the inclination was discussed by KANE (1966) and FERNANDEZ (1967), and recently, ISHII and ELLIS (1970a, 1970b) established a ray-theoretical calculation method for this problem. ROGERS and KISSLINGER (1972), using ray-theoretical transfer functions, obtained the dip angle of the inclination of the Moho interface in some regions.

We should remember that even in the flat-layering case, successful applications of the transfer function are limited to such relatively sharp discontinuities as: the Moho plane at the bottom of the crust and the base boundary of a superficial sedimental layer in the upper crust. Therefore, it is quite reasonable for us to focus solely on the one-layered system in considering the effect of inclination.

Although the problem of lateral heterogeneity or of vertical faults within the crust remains to be solved, the concept of an inclination of a boundary has furthered our understanding of the crustal response. In the area of crustal studies at its present stage of development, model experiments are very useful for demonstrating and summarizing the transfer functions of a dipping layer.

The purpose of this paper is to present experimental examples of the transmission of P or SV waves in a dipping layer with a plane P wave incidence at the base of the layer. An analogous experiment is attempted by ROGERS and KISSLINGER (1972) where the amount of dipping is small. The present paper, however, deals with a large dip angle as well as with a small inclination.

In this model study, the author examines the degree of dip angle at which the flat-layer assumption can be permitted in obtaining the transfer function. In order to examine the validity of the ray theory and detect diffracted waves, there are, in addition to spectral studies, time domain analyses, which utilize travel time curves.

An outline of the present experiment follows: A plane P wave, which represents the input signal, with a certain propagation direction in the lower medium is excited; then it enters the upper medium of the dipping layer; most of the incident energy returns to the lower space after travelling up and down within the layer; while staying there it contributes to the motion at the free surface; measurements are made to detect the output signal, the vertical component of the motion at a certain point of the free surface. The experimental transfer function is defined as the spectral ratio of the output signal to the input signal.

2. *Experimental Method*

In the present study, the major problem is to determine if the ray-theoretical consideration is sufficient for calculating the theoretical transfer function of a dipping layer. Accordingly, the experiment should be conducted under conditions that permit the effect of inclination of the interface upon the rays traveling through the layer to be easily detectable in measurements. This is made possible taking a high contrast of elastic constants and densities between the upper and the lower medium. Then, the interface becomes highly sensitive to the incident wave. The materials selected in this experiment are plexiglas for the upper layer and aluminum for the lower medium as shown in Table 1.

Unfortunately plexiglas shows high anelasticity: in this experiment the attenuation factor Q is estimated to be 30–50 in the frequency range available. This is unfavorable

Table 1. Parameters of the model materials.

	Thickness of the plate (mm)	Density (g/cm^3)	Plate P wave velocity (mm/μsec)	S wave velocity (mm/μsec)	Psudo Poisson's ratio
Aluminum plate	2.0	2.70	5.36	3.08	0.25
Plexiglas plate	1.5	1.19	2.26	1.20	0.30

for a rigorous simulation of a perfectly elastic problem. Nevertheless, an experiment using plexiglas has significance, although a careful examination of experimental data is required. The effect of smoothing an experimental transfer function is one of the evidences of the attenuation.

To clarify the existence of diffracted waves the dip angle is made as large as 45°, although such a large dip might not be realistic in practical problems.

The two-dimensional model consists of three parts: a triangular plexiglas sheet, a triangular aluminum sheet, and an rectangular aluminum sheet all connected together with epoxy adhesive (Fig. 1). The wave emitter is affixed to the rectangular sheet. The propagation direction of the incident wave can be changed by exchanging or removing the triangular aluminum sheet. The dip angle of the dipping layer model is converted by exchanging the triangular plexiglas sheet.

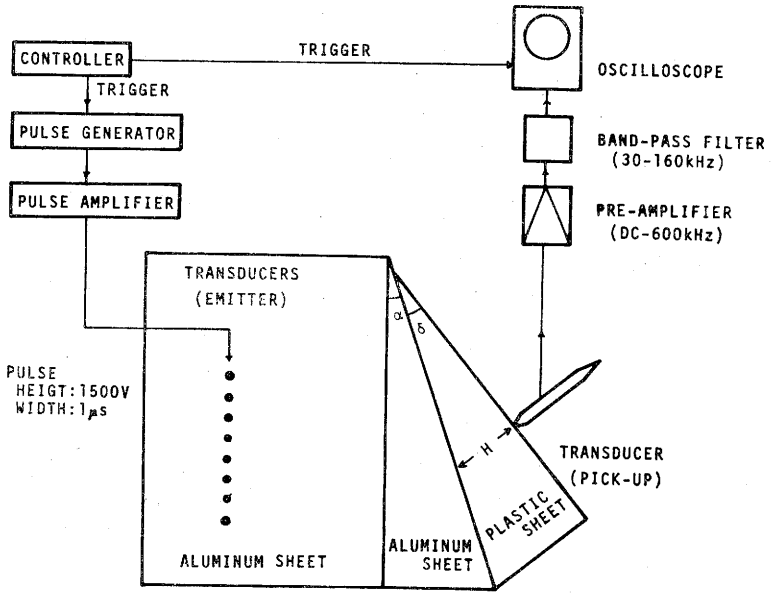

Fig. 1. Diagram of the model and the apparatus.

The linear scales of these sheets are determined in the following way. The source distance of the rectangular sheet, should be large enough to obtain a plane wave. This will be discussed in the next section. Another requirement is to avoid the reverberated coda from the back edge of the sheet. For this purpose the dimension of the sheet is made as large as possible. Eventually the size of the rectangular aluminum sheet is made 80 cm in width and 100 cm in length. Thus the later phases appear more than 80 μsec

after the signal. The dimension of the layer, which is the depth from a certain point at the free surface to the bottom of the layer, is made so that the curve of the transfer function has two or three peaks in the frequency range of the present experiment.

The frequency band is taken as 30–160 kHz so as to reject noises with frequencies lower than 30 kHz or higher than 160 kHz. The latter involves harmonic oscillation of 250 kHz which is the resonant frequency of the wave emitter. The wavelength of P in the plexiglas sheet is between 13 mm and 66 mm.

Since the shortest wave length of P is longer than four times the thickness of both the aluminum and the plexiglas plate, the dispersion of the plate P wave is negligible.

The functions of the apparatus are as follows:

(i) The electric pulse of 1500 V, with a time duration of 1μsec, is excited at the chyratron pulse generator; the time rate of the excitation of the pulses is synchronized by the time controller.

(ii) The controller triggers an oscilloscope.

(iii) The elastic wave is generated by means of the electromechanic transducer (barium titanate transducer).

(iv) The detector is a barium titanate transducer with a brass rod (Fig. 2).

(v) Electric signals are amplified with a gain of 35dB. After amplification they are filtered with a band pass filter and displayed on an oscilloscope.

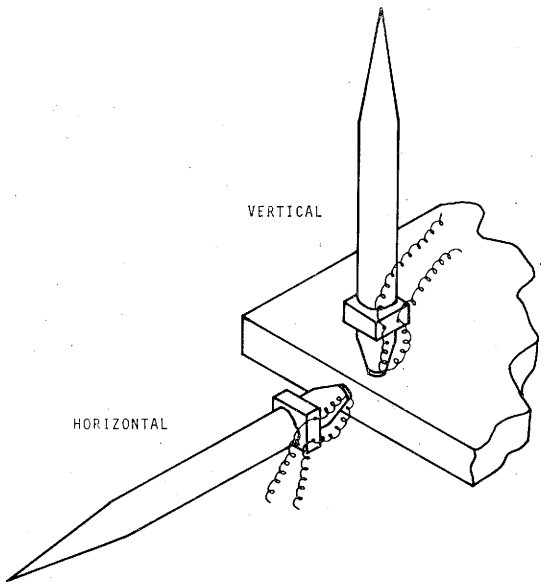

Fig. 2. Receivers for detecting the vibration at the surface and edge of the plate. Only motions perpendicular to the surfaces are detected. The plate surface remains horizontal in this experiment.

In order to make the time scale and the amplitude scale of the data constant throughout the experiments, calibrations of instruments are made for each measurement using standard data; for instance, a record of the incident wave.

As is usual in model studies, scaling or similarity of models should be discussed. For the sake of simplicity let us assume that in the model 1 mm and 1μsec correspond

respectively to 1 km and 1 sec in actual earth. The velocity 1 mm/μsec, therefore, represents 1 km/sec in actual earth, and the frequency 1 MHz corresponds to 1 Hz.

3. *Generation of a Plane Wave*

In order to examine the ray theory, it is essential in this experiment, to generate plane body waves. One simple method is to use the far-field radiation of a source. However, this demands a powerful source and a large size sheet.

I propose another method that is related to Huygens' principle. In two-dimensional space, a plane body wave is considered to be the infinite sum of equal cylindrical waves produced at every point on a straight line. This principle suggests the use of sourses (transducers) that emit cylindrical waves at equal intervals on a line. To decide the number of sources, their spacing, and the range in which the wave is nearly planelike, a numerical simulation is carried out.

Let us take the rectangular cordinate system (x, y). The wave field at (x, y) due to the cylindrical wave sources on the x axis is

$$u=A\cdot\sum_{n=1}^{N} H_0^{(2)}\left(\frac{2\pi\gamma_n}{\lambda}\right)\cdot e^{i\omega t}\ , \tag{1}$$

where $\gamma_n=\sqrt{(x_n-x)^2+y^2}$, x_n is the x cordinate of the n-th source, λ the wave length, ω the angular frequency, N the number of sources, A constant, and $H_0^{(2)}(x)$ the 0-order Hankel function of the second kind. u is rewritten as

$$u=U(x, y, \lambda)\cdot e^{i\omega t-i\cdot 2\pi/\lambda\cdot y+i\phi(x,y,\lambda)}\ , \tag{2}$$

where $U(x, y, \lambda)$, $\phi(x, y, \lambda)$ denote the spectral amplitude and the reduced phase angle at (x, y), respectively. A homogeneous plane wave requires that U and ϕ be independent of x, y, and λ.

Figure 3 shows the amplitude distributions of u for eleven sources with various interval of sources a. The wavelength of the cylindrical wave in the medium is taken as a unit of x (the 6-th source is situated at $x=0$), y, and a. The variations of ϕ versus x are given in Fig. 4 for $a=0.5$, $a=1.0$ and $a=1.5$.

As Fig. 3 and Fig. 4 indicate, the source interval should be smaller than the wave length so as to obtain a uniform distribution of the amplitude and the phase angle. The plot of the maximum amplitude for every y is shown in Fig. 5. The attenuation curve approaches to that of the case where the source is single, or proportional to $1/\sqrt{y}$, as the interval of sources becomes greater than the wavelength.

Because the interval of sources should be less than the wavelength, let us adopt 0.75 in units of the wavelength as the upper limit of the length of the source interval. In this case, the distance between the source and the pick up is approximately fifteen times larger than a wave length in order to obtain a plane wave.

In the present experiment, the number of sources is 10, their interval is 15 mm, and the distance from the sources to the boundary between the rectangular aluminum sheet and the triangular sheet is 500 mm, taking account the minimum wavelength available in the aluminum plate, i.e., 20 mm, corresponds to 250 kHz, the resonant frequency of the emitting transducer. The sources, cylindrical barium titanate transducers buried in the aluminum plate, excite cylindrical plate P waves.

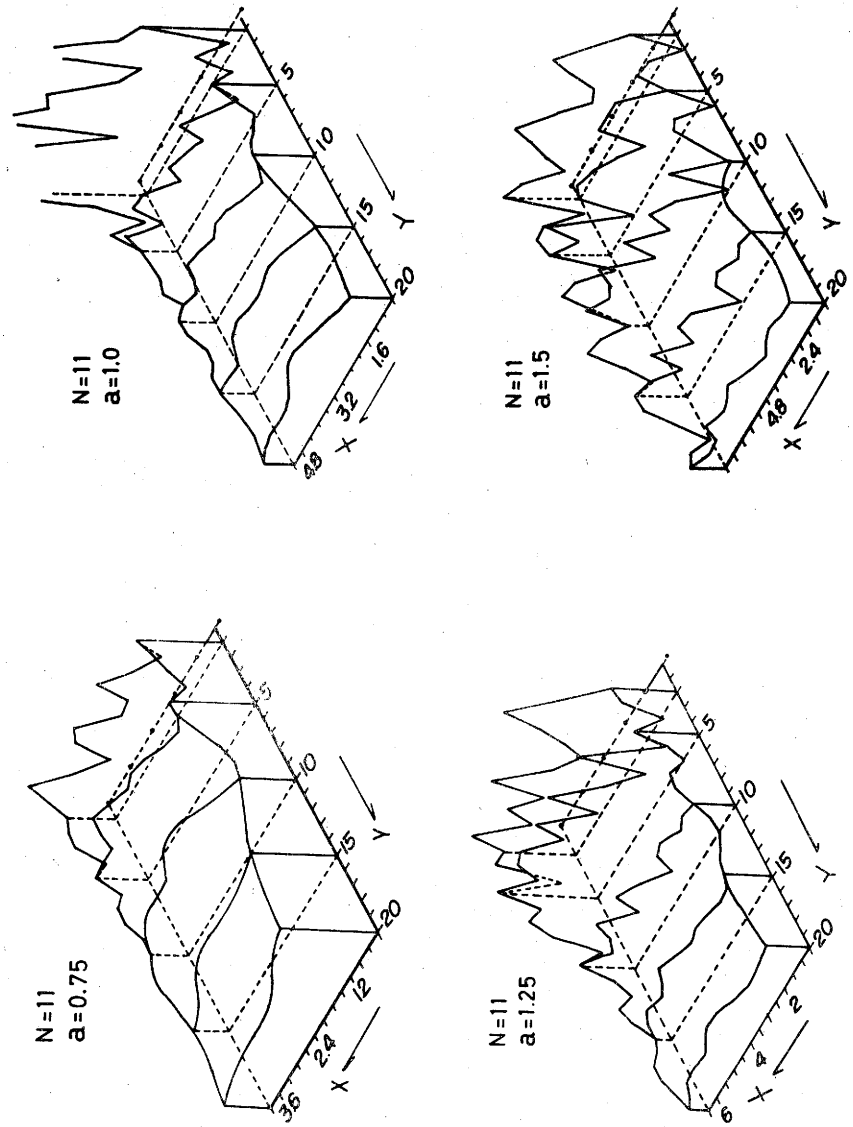

Fig. 3. Amplitude distribution of a theoretical wave field with superposed cylindrical waves for a given wavelength.

The number of cylindrical wave sources is 11; the 6-th source is located at $(x, y)=(0, 0)$. The wavelength is taken as a unit of the distance, including the interval of the sources a.

We can obtain the amplitude distribution of the generated plate P wave by measuring the motions at the aluminum plate surface.* The vertical component of the motion at the horizontal plate surface is detected by the vertical receiver, Fig. 2. The

* The amplitudes of the two-dimensional motions parallel to the plate surface are proportional to those of the motions perpendicular to this surface for a given frequency.

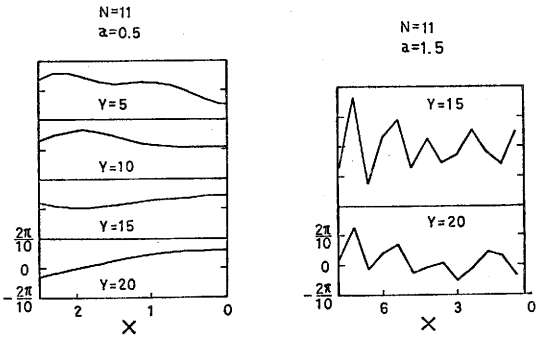

Fig. 4. Distribution of the reduced phase angle of a theoretical wave field with superposed cylindrical waves for a given wavelength.
The parameters are the same as in Fig. 3.

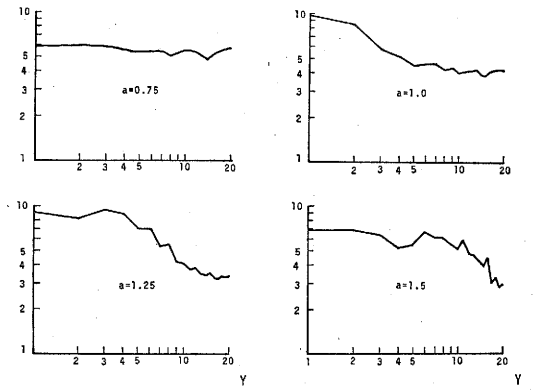

Fig. 5. Attenuation of the maximum amplitude for every y.

results are shown in Fig. 6 and Fig. 7 for the prominent wave length 40 mm and 20 mm, respectively. We find that the experimental distribution of the amplitude of these superposed cylindrical waves may be regarded as that of a plane wave.

4. *Experimental Transfer Functions*

In this section, the spectral behavior of surface motions due to elastic waves incident to a dipping layer will be discussed in relation to experimental transfer functions of the layer, which are the spectral ratios of the vertical components of the surface motions to the wave motions of the incident plane wave. The incident wave is detected at the upper boundary of the lower medium (aluminum plate) before the layer model is attached to the boundary.

The oscillograms of the detected waves are digitized at every 0.6μsec; the interval of the discrete frequencies is 0.0033 MHz and the Nyquist frequency is 0.833 MHz. In order to correct for errors due to fluctuations in the time scales of the wave traces, the frequency scale, is changed. Thus, a frequency scale with an accuracy of higher than 3% is obtained.

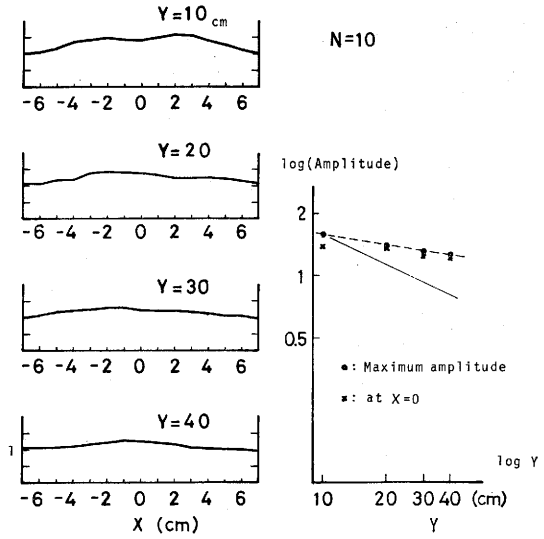

Fig. 6. Experimental data of the amplitude distribution of the incident wave field for a prominent wave length of approximately 40 mm, and its decay curve. The solid line indicates the geometrical spreading of an isolated source of a cylindrical wave.

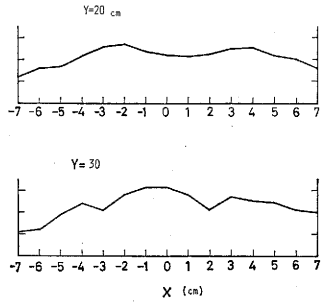

Fig. 7. Experimental data of the amplitude distribution of the incident wave for a prominent wave length of approximately 20 mm.

Although the accuracy of the relative amplitudes of the experimental transfer functions is maintained at 5–10%, the absolute value of the transfer functions has not been accurately determined.

The notations of the parameters of the model are defined as follows: α angle of incidence measured from the normal to the interface; δ dip angle; H depth measured along the normal perpendicular to the free surface down to the interface. The signs of δ indicate two possible configurations of the layer model, as illustrated in Fig. 8.

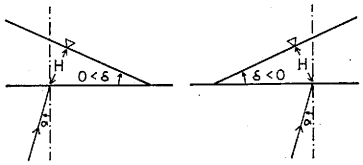

Fig. 8. Illustration of the model parameters. α: incident angle, δ: dip angle, H: depth to the interface.

The amplitude characteristics of the experimental transfer functions for various dip angles are summarized in Fig. 9 and Fig. 10, when $\alpha=0°$, and $\alpha=30°$ respectively. In addition to the transfer functions, the spectral amplitudes of the vertical component of the surface motions when $\alpha=10°$ are presented in Fig. 11. This will also give us the same quality of information about the characteristics as the normalized spectra, because the spectrum of the incident wave has no peculiar peaks or troughs.

By studying these figures, we notice some important features of the transfer function for a dipping layer. In order to classify the characteristics of the transfer functions with respect to dip angle, let us divide the range of a dip angle into three parts: 0° to

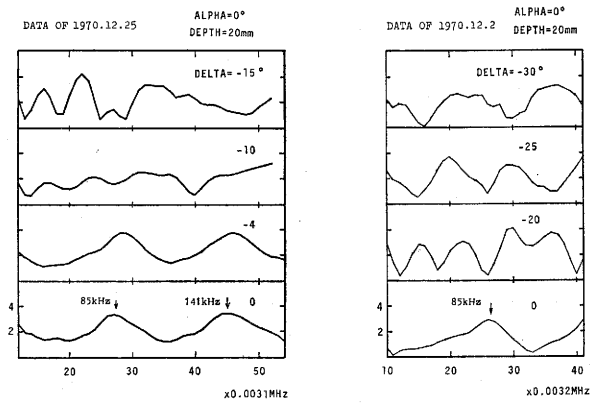

Fig. 9. Amplitude characteristics of the experimental transfer functions for $\alpha=0°$.

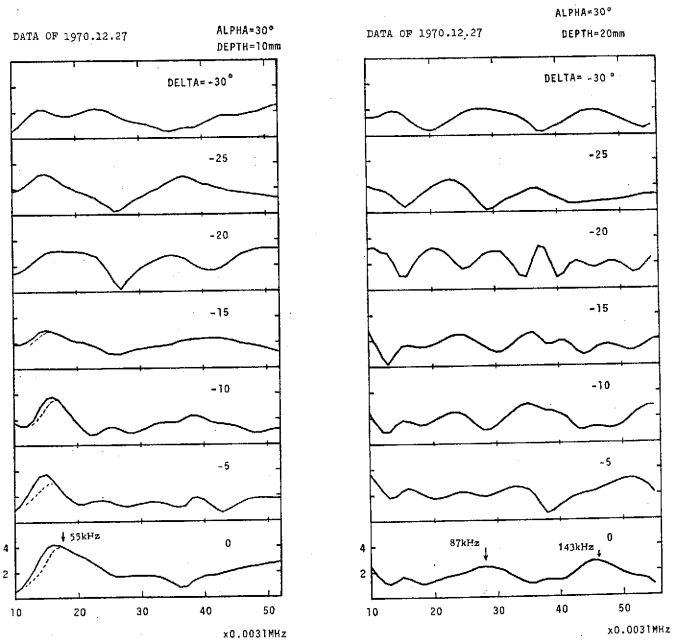

Fig. 10. Amplitude characteristics of the experimental transfer functions for $\alpha=30°$.

10°, 10° to 20°, and the range larger than 20° when $\alpha=0°$. This classification should be altered according to the value of α and to the frequency band under consideration.

The first range (0° to 10°) is characterized by small amount of the effect of the inclined interface; only a slight shift of peaks in the characteristic is observed as compared to the case where the horizontal layer has the same depth to the interface as that of the dipping layer. The flat-layer approximation to the crustal model is valid for applying the theoretical transfer functions to practical problems in seismology.

When the range is 10° to about 20°, the characteristic curve changes greatly. This

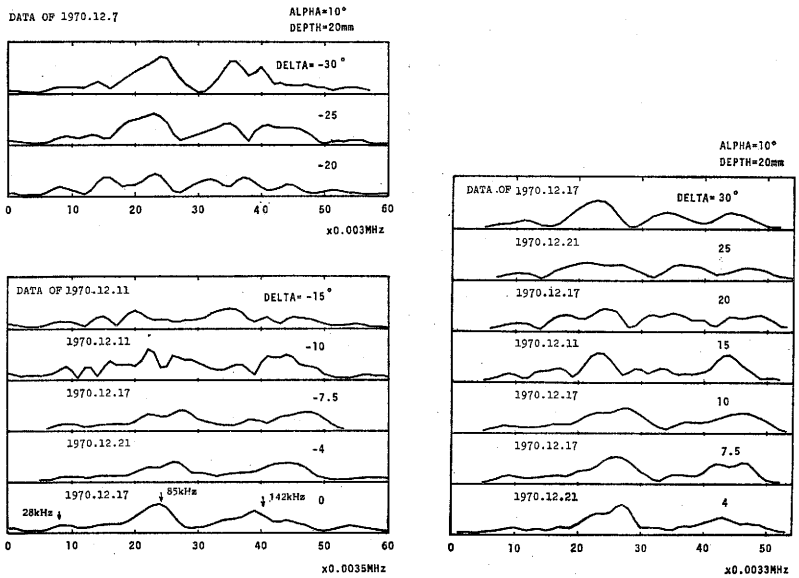

Fig. 11. Amplitude characteristics of the spectra of the waves detected at the free surface of the layer for $\alpha=10°$.

implies complexity of multiple reflection: the rays in the layer may have various propagation directions, and conversion between P and SV waves may occur intensively. In the time domain, the reflected pulses are not clearly identified, as can be seen in Fig. 12 where $\alpha=30°$. Therefore, the behavior of the elastic waves propagating within the moderately dipping layer, whose dip angle is between 10° to about 20°, should be discussed in the frequency domain treated in this section rather than in the time domain to be discussed later.

In the third range, we find that the characteristic resembling that of the first range, tends to show a rather simple shape. This stems from the fact that the rays are apt to spread far from the vertex with few reflections at the free surface and the interface. As shown in Fig. 12, the amplitude of a reflected pulse is quite large. Such waves are converted S phases and will be confirmed in the next section.

The experimental transfer functions examined in this section are based on the assumption that the incident wave is almost planelike. In a previous section, we discussed how a plane wave is obtained in the lower medium (aluminum plate). The predominant waves in the plexiglas layer were found to be plane waves. As shown in Fig. 13, the transmitted waves observed at the free surface of the layer model for a flat layer also indicate that the waves in the layer can be regarded as plane waves with respect to their wave forms and the arrival times of their energies.

Moreover, the difference due to the anelasticity between the experiment and the theory of elasticity should be taken into account when interpreting the experimental transfer functions. The theoretical transfer function for $\alpha=30°$, $\delta=0°$ is shown in Fig. 14. The corresponding experimental transfer function is given in Fig. 10. The peaks in the characteristic curve are much steeper than those of the transfer function which were obtained through analysing the experimental data.

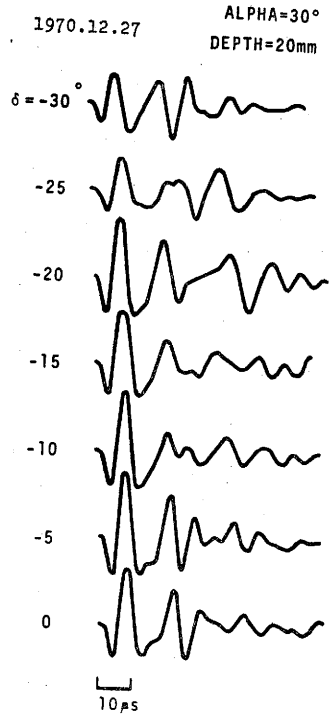

Fig. 12. Wave traces detected at the free surface of the layer for $\alpha=30°$.

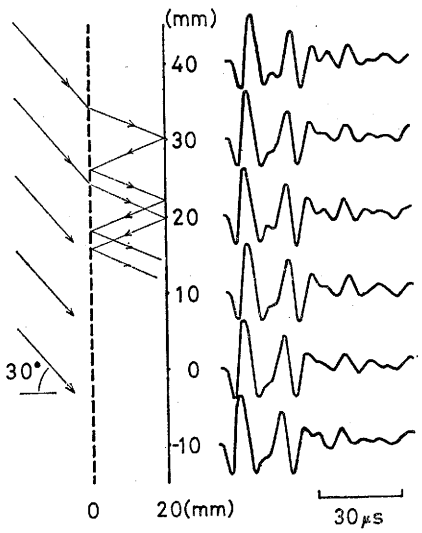

Fig. 13. Wave traces detected at the free surface for $\alpha=30°$, $\delta=0°$.

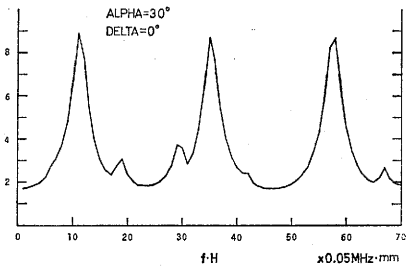

Fig. 14. Amplitude characteristic of the theoretical transfer function for $\alpha=30°$, $\delta=0°$.

The elastic constants and the model parameters are as the same as the experiment.

5. *Time Domain Analysis*

In this section, the treatment is restricted to where $\alpha=0°$, and dip angle is greater than 20°, for the sake of simplicity.

Figure 15 dipicts multiple reflections within a dipping layer and wave forms detected both at the free surface and at the plate surface along the medial line of the wedge when $\delta=45°$ Distance is measured from the apex and the origin time is defined as the arrival time of the maximum amplitude of the incident P wave at the bottom of the dipping layer. The form of incident wave is observed at the apex, i.e., $x=0$ cm. The solid and the broken lines, determined by a graphical method, the travel time curves of P phases and S phases respectively. It should be noted that the vertical component of the wave motion at the plate surface, (b) in Fig. 15, does not involve S phases.

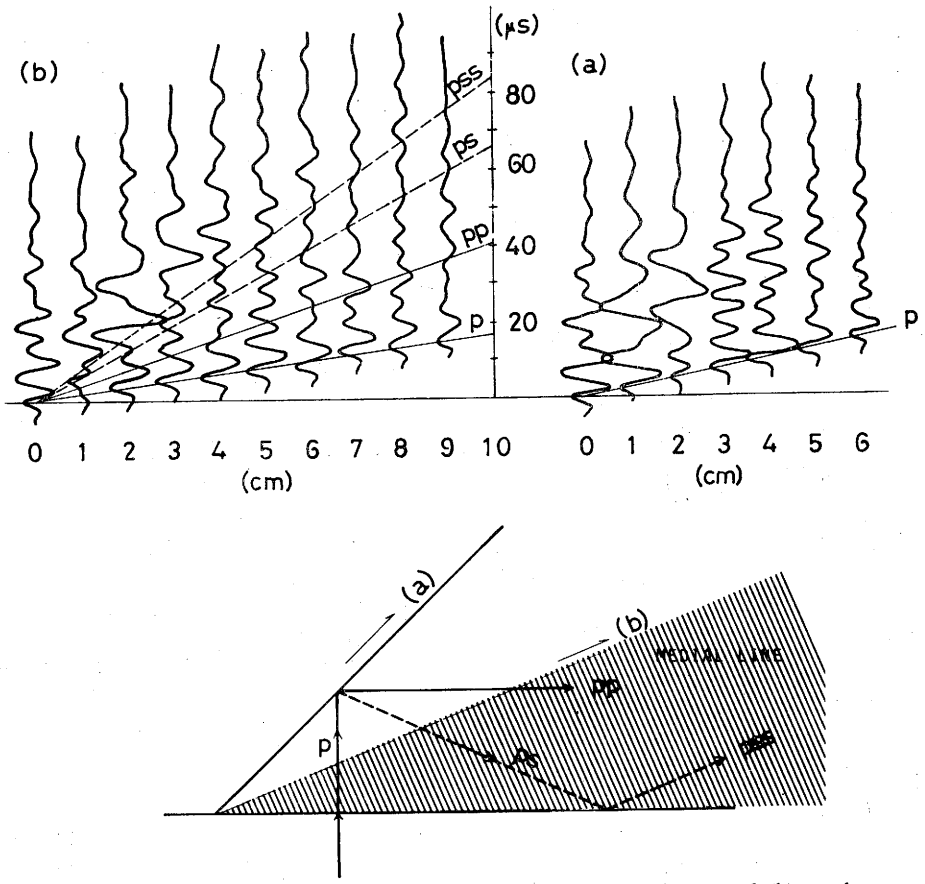

Fig. 15. Wave traces detected (a) at the free surface of the layer and (b) at the plate surface along the medial line of the wedge for $\alpha=0°$, $\delta=45°$.

A travel time curve (a line passing through the original point of the coordinate system) is drawn for every theoretically expected ray phase. The solid and the broken lines indicate P and S phase respectively. The hatched area within the layer is the illuminated zone of PSS.

In Fig. 15 we observe ray-theoretically unexpected waves of relatively large amplitude. These diffracted waves are associated with PSS (rays, reflected and converted to S phase at the free surface and again reflected at the bottom of the layer) which propagates without colliding with the free surface (Fig. 15). Such diffracted waves spread out of the ray-theoretically defined region of the PSS that is indicated by the shaded area in Fig. 15.

Where the dip angle is great, diffraction due to a prominent outgoing ray is so remarkable that the ray theory is insufficient for calculating the wave field. However, it is expected that the intensity of such outgoing rays, and thus, the diffraction, is weakened when there is multiple reflection for smaller dip angles.

Let us examine the wave forms at the free surface of the layer (the edge of the plate) as shown in Fig. 16. For a dip angle of 36.4°, PSS is propagated parallel to the surface. Beyond this angle, there is much diffraction. The arrival times of ray-theoretical phases shown in the same manner as in Fig. 15, coincide with those of the waves detected in the seismograms, except for the minor waves. This indicates that the plane waves in this experiment are almost perfect. It is remarkable that the converted S phases are prominent; their polarity can be understood by using the principle of reflection.

By observing the motion at some point within the layer, i.e., detecting the motion at the plate surface of the model, we can examine the diffraction effect. In Fig. 17 the wave forms, detected at the plate surface along the medial line, are compiled with travel time curves of rays. Anomalous waves, arriving after ray-theoretical waves, are found in the vicinity of the vertex; they decay rapidly as they move away from the apex of the wedge.

It is doubtful that all of these waves come from a two-dimensional diffraction effect, since coupling between M_{11} or plate P wave and M_{21}, for instance, may occur owing to the incompleteness of the two-dimensional model construction. Near the vertex, the dimension of the vertical cross section of the wedge is comparable to that of the free surface, the thickness of the model plate.*

In any case, the anomalous waves can be neglected when observing at the free surface, if we take the signal to noise ratio of the record to be about 20dB.

It may be concluded that the diffraction effect is negligible if the dip angle is so small that the outgoing rays are not prominent. The diffraction effect should be evaluated by calculating the intensity of these outgoing ray-theoretical waves. ISHII and ELLIS (1970a, b) calculated the discontinuity of the displacement due to such waves.

6. *Concluding Remarks*

The present model study reveals the nature of elastic waves propagated through a dipping structure.

In the study of the transfer functions, the range of dip angle can be divided into three parts: for the small dip angle, the shape of the characteristic curve is almost the same as in the case of a horizontal layer, showing a slight shift of the peak frequencies in the characteristic with dip angle; in the case of a moderate dip angle, the complexity

* In two-dimensional model experiments, model plates are usually regarded as sufficiently thin.

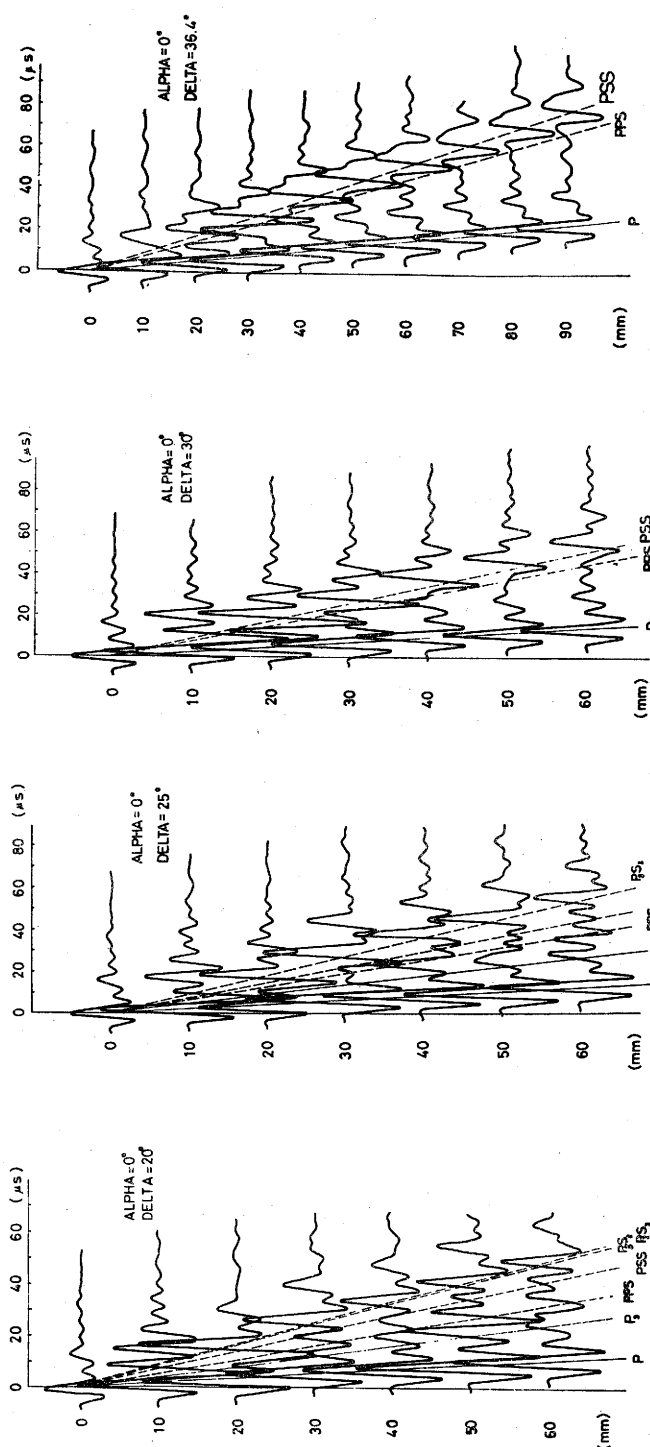

Fig. 16. Wave traces detected at the free surface of the layer (the edge of the plate) for $\alpha=0°$ with various dip angles. The travel time curves are drawn in the same way as in Fig. 15.

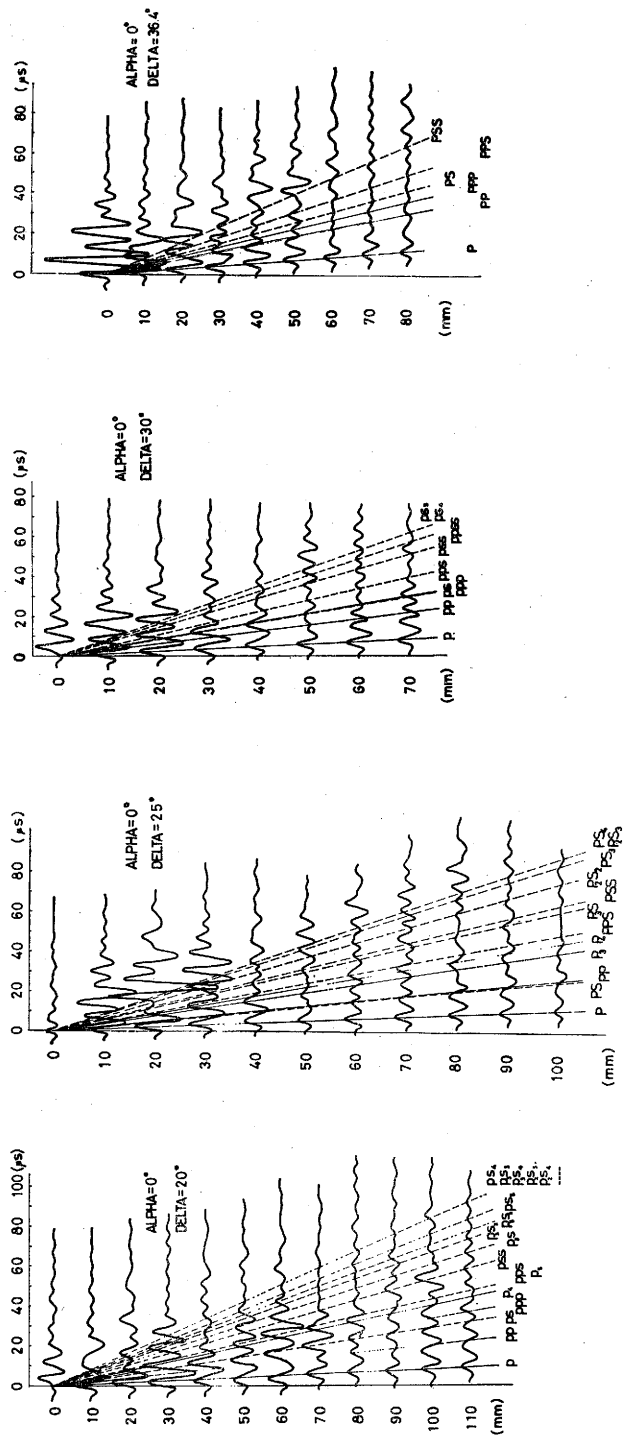

Fig. 17. Wave traces detected at the plate surface along the medial line of the wedge for $\alpha=0°$ with various dip angles. S phase are not detected in this case; the vertical receiver in Fig. 2 is employed. The travel time curves of main phases are drawn.

of the curve is eminent; for a large dip angle, the curve resembles that of a small dip angle. Above nature is also found in the theoretical study of ISHII and ELLIS (1970b).

In the study of wave forms, there is a diffraction effect for a large dip angle, discriminating multiply reflected rays with relatively large amplitude, which are identified by the use of travel time curves of ray-theoretical phases.

In this experimental study, the generation of a plane wave, accomplished by superposing many cylindrical waves, plays an essential role. Numerical simulation indicates that the interval of sources should be less than the wavelength under consideration. The generated wave is examined in the preliminary experiment: measurements are made of the amplitude distribution and the phase lag of the emitted pulse.

The above experimental technique can be applied to other problems in model seismology. Plane wave are sometimes quite easy to handle in theoretical considerations; therefore accurate comparisons between theory and experiments are possible if we use plane waves in experiments.

The author wishes to express his sincere thanks to Professors Toshi ASADA and Ryosuke SATO for their encouragement and helpful advice during the course of this study. The expense of the present study was defrayed by Grant in Aid for Scientific Research, the Ministry of Education of Japan.

REFERENCES

FERNANDEZ, L. M., Master curves for the response of layered systems to compressional seismic waves, *Bull. Seism. Soc. Amer*, **57**, 515–543, 1967.

ISHII, H. and R. M. ELLIS, Multiple reflection of plane SH waves by a dipping layer, *Bull. Seism. Soc. Amer*, **60**, 15–28, 1970a.

ISHII, H. and R. M. ELLIS, Multiple reflections of plane P and SV waves by a dipping layer, *Geophs. J.*, **20**, 11–30, 1970b.

KANE, J., Teleseismic response of a uniformly dipping crust, *Bull. Seism. Soc. Amer.*, **56**, 841–859, 1966.

PHINNEY, R. A., Structure of the Earth's crust from spectral behavior of long period body waves, *J. Geophys. Res.*, **69**, 2997–3018, 1964.

ROGERS, A. M. Jr. and C. KISSLINGER, The effect of a dipping layer on P-wave transmission, *Bull. Seism. Soc. Amer.*, **62**, 301–324, 1972.